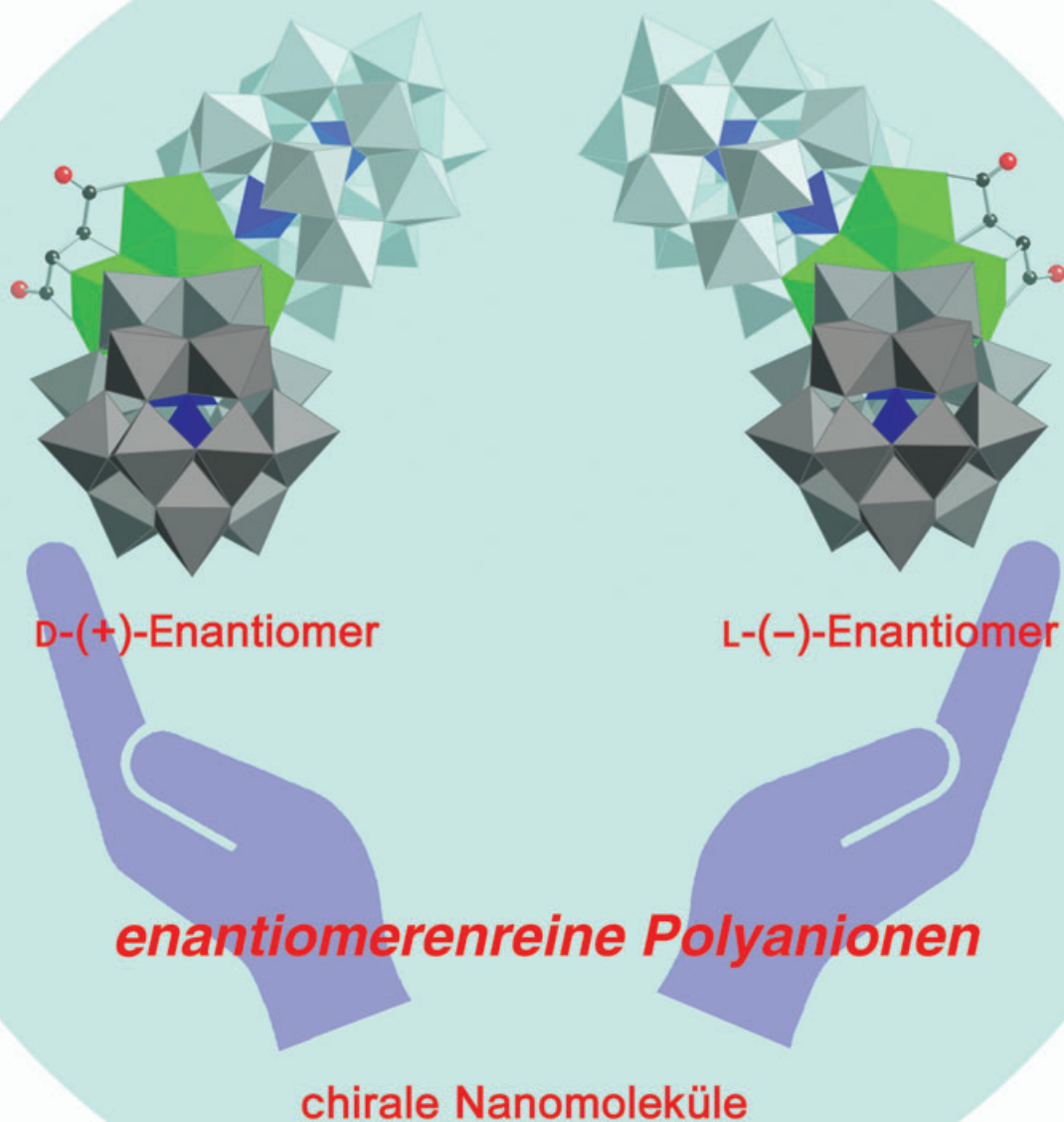


# Zuschriften



Der Chiralitätstransfer von dem kleinen organischen Naturstoff Tartrat auf ein mehrere Nanometer großes Polywolframat führt zu den reinen Enantiomeren des nichtlabilen Polywolframats. Weitere Informationen zu dieser vielversprechenden Strategie enthält die Zuschrift von C. L. Hill et al. auf den folgenden Seiten.

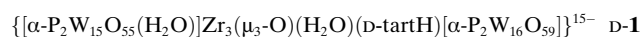
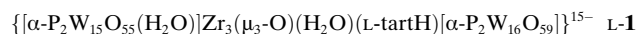
## Chirality Transfer

## Enantiomerically Pure Polytungstates: Chirality Transfer through Zirconium Coordination Centers to Nanosized Inorganic Clusters\*\*

Xikui Fang, Travis M. Anderson, and Craig L. Hill\*

Stable, nanometer-sized enantiomerically pure polyoxoanions could lead to useful chiral materials ranging from microporous solids and inorganic pharmaceuticals to catalysts for homogeneous asymmetric oxidation. However, chirality has been largely unexplored in polyoxometalate (POM) systems.<sup>[1]</sup> Most POMs with chiral structures undergo rapid racemization in solution, and racemic mixtures are usually seen in solution as well as in the solid state. Typically in crystals the two enantiomers coexist in the same unit cell, related to each other by a crystallographically imposed inversion center.<sup>[2]</sup> Although Pfeiffer effects have been demonstrated with a wide range of racemic POM systems, the chiral resolution of the enantiomers is frequently complicated by their solubility, lability, and structural similarity.<sup>[3,4]</sup> Three different synthetic routes to enantiopure POMs in the solid state have been reported. First, hydrothermal synthesis can produce solid inorganic materials with helical characters.<sup>[5]</sup> One example is the vanadium phosphate complex,  $[(\text{CH}_3)_2\text{NH}_2]_4[\text{V}_{10}\text{O}_{10}(\text{H}_2\text{O})_2(\text{OH})_4(\text{PO}_4)_7] \cdot 4\text{H}_2\text{O}$ , with a chiral interpenetrating double helix of Zubieta and co-workers.<sup>[5a]</sup> Second, reactions of a few polymolybdates and chiral amino acids afford chiral POMs.<sup>[6]</sup> A recent study by Kortz et al. demonstrated that the bound amino acids are probably labile in solution, based on NMR spectroscopy and X-ray studies (weak bonding, approximately 2.3 Å, between the Mo and carboxylate O atoms).<sup>[6b]</sup> Therefore it is not surprising that the chirality of these complexes is largely localized on the amino acid moieties. Third, counterions can play a critical role in determining the solid-state structures of POMs, and, in some cases, cause achiral POMs to crystallize in chiral space groups.<sup>[7]</sup> Sometimes crystallization of racemic bulk solids can lead to chiral crystals.<sup>[8]</sup> However, there is no report of chiroptical activity in the solution-state for such enantiopure POM systems. Realization of an intrinsically chiral and configurationally stable POM should afford enantioselective catalytic properties and enhanced biological activities.<sup>[9]</sup> Furthermore, the control of chiral induction is an important component of the larger goal of effectively managing and utilizing chirogenic phenomena.

Herein we report the synthesis and characterization of chiral, nonracemizing, enantiomerically pure polyoxotungstates, **L-1** and **D-1** prepared in bulk. Significantly, strong



chiroptical effects are manifested by the POM units as a result of chirality transfer from a far smaller enantiopure organic molecule, L- or D-tartaric acid ( $\text{HO}_2\text{CCH}(\text{OH})\text{CH}(\text{OH})\text{CO}_2\text{H}$ ; L-tartH<sub>4</sub> or D-tartH<sub>4</sub>). Both enantiomeric complexes have been characterized by elemental analysis, <sup>31</sup>P NMR, IR, and UV/Vis spectroscopy, in addition to the single-crystal X-ray structure analysis on the L enantiomer, and their solution chiroptical properties have been demonstrated by circular dichroism (CD) spectroscopy.

The synthetic approach involves recognition between an achiral host and chiral (nonracemic) guest molecule to produce a chiral microenvironment on the achiral host, a phenomenon revealed by induced circular dichroism (ICD).<sup>[10]</sup> This straightforward strategy, outlined in Figure 1,

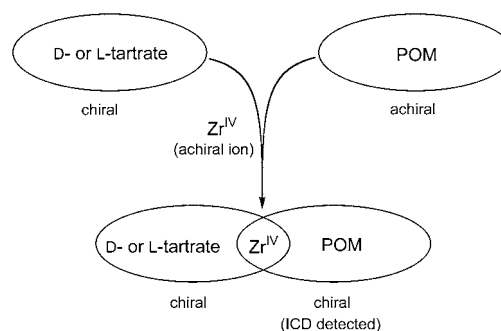


**Figure 1.** The interaction between D- or L-tartrate and the achiral POM unit through the coordinated  $\text{Zr}^{\text{IV}}$  ions.

relies on the “recognition” between  $\alpha\text{-}[\text{P}_2\text{W}_{15}\text{O}_{56}]^{12-}$  (**2**), an achiral lacunary Wells–Dawson POM unit of  $C_{3v}$  symmetry, and the simple  $C_2$ -symmetric D- or L-tartrate ligand.<sup>[11]</sup> Given the electrostatic repulsion between **2** and tartrate, a positively charged mediator is needed for chirality transfer. The  $\text{Zr}^{\text{IV}}$  ion, is well suited for this task because it has both high charge density and coordination flexibility.<sup>[12,13]</sup> In the systems reported herein, the  $\text{Zr}^{\text{IV}}$  ions transmit chirality from the chiral tartrate to the polytungstate units by binding strongly to both.

This approach facilitates the crystallization of **L-1** in the chiral orthorhombic space group  $P2_12_12_1$ , with only one enantiomer present in the unit cell ( $Z = 4$ ). Crystallization in a chiral space group is a rare but ideal starting point for the generation of chiral materials. The structure of **L-1** consists of two units of **2** bridged by a central fragment containing three  $\text{Zr}^{\text{IV}}$  centers and one  $\text{W}^{\text{VI}}$  center (Figure 2a). All three zirconium atoms are nonequivalent and form a triangular unit sharing a coplanar  $\mu_3$ -oxo oxygen atom. One of the zirconium atoms,  $\text{Zr3}$ , serves as a “hinge” between the two  $\alpha\text{-}[\text{P}_2\text{W}_{15}\text{O}_{56}]^{12-}$  units, while the other two zirconium ions ( $\text{Zr1}$

[\*] X. Fang, Dr. T. M. Anderson, Prof. Dr. C. L. Hill  
Department of Chemistry  
Emory University  
1515 Dickey Drive, Atlanta, GA 30322 (USA)  
Fax: (+1) 404-727-6076  
E-mail: chill@emory.edu

[\*\*] We gratefully acknowledge the National Science Foundation (Grant CHE-0236686) for funding the research, and Grant CHE-9974864 for funding the D8 X-ray instrument.

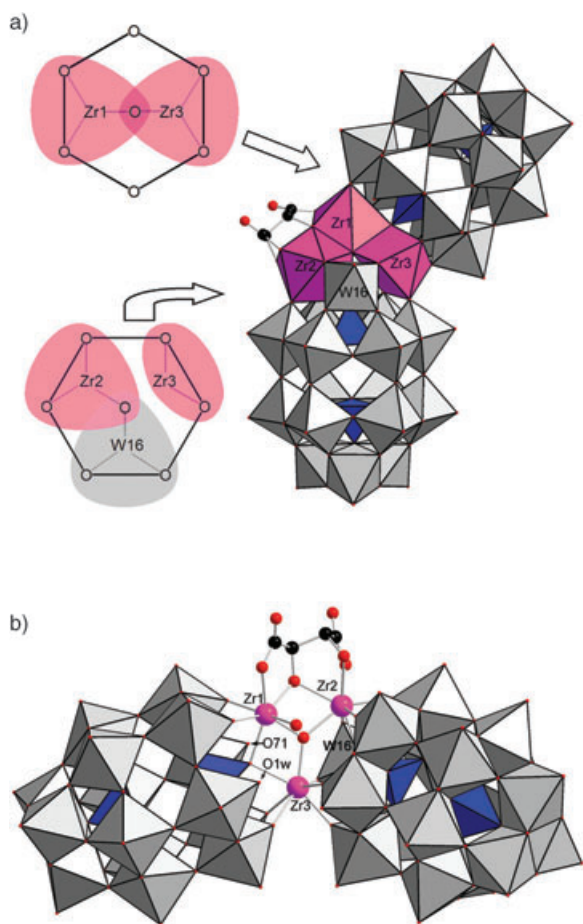
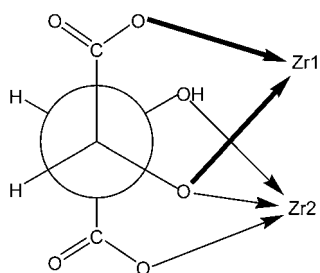


**Figure 2.** The structure of L-1. a) A combination ball-and-stick/polyhedral representation of L-1 with the metal-oxide framework in polyhedral notation and the L-tart ligand in ball-and-stick notation; gray W, blue P, purple Zr, black C, red O. The hexagons illustrate the coordination between substituted Zr or W sites with the seven terminal oxygen atoms in the vacant positions of the polytungstate moieties. b) A side view of L-1 showing the three Zr centers as well as the L-tart ligand in ball-and-stick representation.

and Zr2) are bridged by the L-tart unit, by chelation through both the hydroxy and carboxy groups in an unusual  $\eta^2:\mu_1:\mu_2:\mu_1:\mu_1$  fashion (Scheme 1).<sup>[14]</sup> Bond valence sum calculations reveal that one of two “hydroxy” oxygen atoms on L-tart remains protonated while the other, which bridges the two Zr centers, does not. The asymmetric protonation reduces the local symmetry of the L-tart unit from  $C_2$  to  $C_1$ . This mixed protonation state is very rarely observed in metal tartrate



**Scheme 1.** The coordination environment of the L-tart ligand in L-1.

complexes,<sup>[14a]</sup> and is likely a key factor in providing the strong complexation between L-tart and the large metal-oxide framework. This complexation in turn dictates the configurational stability of L-1. In other words, the protonation state of the L-tart hydroxy groups adjusts in response to rearrangements in the coordination sphere of the zirconium ions caused by the ligation of 2. Simultaneously the chelating L-tart maintains the enhanced complexation ability provided by the vicinal hydroxy oxygen atoms.

Two of the three vacant positions in the bottom  $\alpha$ -[P<sub>2</sub>W<sub>15</sub>O<sub>56</sub>]<sup>12-</sup> (2) unit shown in Figure 2a are occupied by zirconium ions, Zr2 and Zr3, and each bridges a pair of adjacent corner-sharing W octahedra in 2. A tungsten atom (W16) is located in the third position, presumably from the decomposition of 2 in the acidic solution. In contrast, the top unit of 2 remains coordinatively unsaturated, which provides an energetically favorable coordination geometry about the zirconium ions (see the hexagonal schematics in Figure 2a). The top unit is rotated with respect to the bottom unit about the central rotation axis running through the two P atoms by about 60° such that only two vacant positions are occupied in a diagonal fashion by two zirconium ions, Zr1 and Zr3. This leaves two of the seven “ligating” oxygen atoms of 2 uncoordinated. Thus the entire framework of L-1 exhibits no local symmetry in either the organic or inorganic moieties. The asymmetry of the L-tart ligand is extended to the POM structure by the zirconium ions, making L-1 a topologically chiral species. It is also of note that the two uncoordinated terminal oxygen atoms in the top 2 unit mentioned above are also different from one another in L-1 (Figure 2b). One of them is replaced by an aqua ligand O1w (W–OH<sub>2</sub> ca. 2.25 Å) while the other atom (O71) remains unprotonated (W=O ca. 1.76 Å).

The <sup>31</sup>P NMR (162 MHz, D<sub>2</sub>O) spectrum of L-1 shows four signals ( $\delta$  = –6.29, –6.62, –12.88, and –13.83 ppm) and the spectrum remains unchanged for several weeks, indicating that the  $C_1$  symmetry exhibited by the solid-state structure (Figure 2) exists and persists in solution. These spectral data also preclude the presence of any diastereomers. The chirality of L-1 is also demonstrated unambiguously by its solution-state optical properties. This optically active complex shows a negative optical rotation in contrast to the free L-(+)-tartaric acid precursor. As seen in Figure 3, the profile of the CD spectrum of L-(–)-1 is totally different from that of its precursor, L-tartaric acid (Figure 3, inset), which only shows a single negative Cotton effect at 214 nm. In the long-wavelength spectral region where L-(–)-1 is CD-active (above 240 nm; vertical dashed line in the inset), L-tartaric acid is almost CD silent. In contrast, L-(–)-1 exhibits strong Cotton effects up to 350 nm, the spectral region where the characteristic oxygen-to-tungsten charge-transfer bands of both plenary and the lacunary Wells–Dawson polyanions occur.<sup>[15]</sup> These results clearly show the ICD in the metal-oxide cluster moiety. Recently, a systematic study of intrinsic circular dichroism in L-tartaric acid and its salts established that the magnitude ( $\Delta\epsilon$ ) of their CD spectra never exceeds 5 dm<sup>3</sup> mol<sup>–1</sup> cm<sup>–1</sup> in the absorption region below 220 nm.<sup>[16]</sup> In contrast, the observed high ICD intensity for L-(–)-1 suggests a moderately strong induced chirality. Thus the

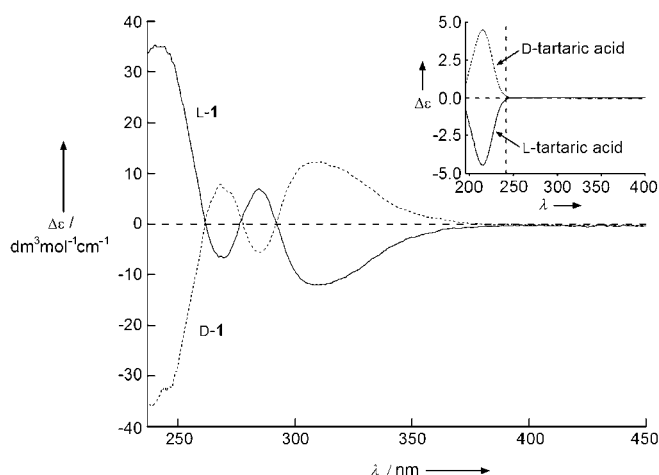


**Figure 3.** CD spectra of both the L-(–)- and D-(+)-enantiomers of **1** and their precursors, L-(+)- and D-(–)-tartaric acids (inset, the same scale units apply) as aqueous solutions. See text for details.

asymmetric arrangement of the zirconium ions in the substituted positions and the lowering of symmetry on the POM ligands facilitate transfer of chirality from L-tart to the POM, and the induced optical activity in **1** is quite pronounced. There is no detectable change in optical activity of L-(–)-**1** with time, again indicating no racemization of the enantiomeric complex in solution.

Significantly, the other enantiomer of the complex, D-**1**, can be prepared from the unnatural D-tartaric acid under synthetic conditions otherwise identical to those used in the preparation of L-**1**, and it exhibits the same physical and spectroscopic properties as L-**1** except for the chiroptical behavior. Although we were not able to obtain diffraction-quality crystals of D-**1**, the mirror-symmetrical CD spectra for L-(–)-**1** and D-(+)-**1** (Figure 3) confirm they are enantiomers of one another.

In conclusion, we have prepared and purified both enantiomers of a polytungstate. Chirality from a small organic ligand, tartrate, can be transferred to a much larger (ca.  $2 \times 1 \times 1$  nm) metal–oxide cluster through high-coordinate zirconium centers. The metal-substituted POM units in the two enantiomers show significant induced circular dichroism. The complexes are stable with respect to racemization, other rearrangements, and decomposition, a key point for applications in catalysis, material science, and applied biology.

## Experimental Section

Preparation of  $[(\text{CH}_3)_2\text{NH}_2]_{15}(\text{L-1}) \cdot 25 \text{H}_2\text{O} \cdot \text{ZrO}(\text{NO}_3)_2 \cdot 6 \text{H}_2\text{O}$  (0.24 g, 0.7 mmol) was dissolved in  $\text{H}_2\text{O}$  (15 mL). L-Tartaric acid (0.105 g, 0.7 mmol) was then added to the stirred solution, resulting in a slurry. Solid  $\text{Na}_{12}[\alpha\text{-P}_2\text{W}_{15}\text{O}_{56}] \cdot 18 \text{H}_2\text{O}^{[17]}$  (1.00 g, 0.23 mmol) was added to the mixture in one portion with vigorous stirring. After 30 min at room temperature, a clear solution resulted to which dimethylamine hydrochloride (0.4 g, 5 mmol) was added. The solution was then heated to  $70^\circ\text{C}$  for 15 min. Slow evaporation of the solution produced needle-like crystals after 24 h (yield 0.51 g, 49.5%). Elemental analysis: calcd Zr 2.96, P 1.34, W 61.55; found Zr 3.08, P 1.40, W 63.38.  $[(\text{CH}_3)_2\text{NH}_2]_{15}(\text{D-1}) \cdot 29 \text{H}_2\text{O}$  was prepared in the same way except that D-tartaric acid was used instead of L-tartaric acid (yield

0.48 g, 46.4%). Elemental analysis: calcd Zr 2.93, P 1.33, W 61.07; found Zr 3.01, P 1.42, W 60.25. The number of crystal water molecules was determined by thermogravimetric analysis (TGA).

X-ray analysis and crystal data for L-(–)-**1**,  $[(\text{CH}_3)_2\text{NH}_2]_{15}[\alpha\text{-P}_2\text{W}_{15}\text{O}_{55}(\text{H}_2\text{O})]\text{Zr}_3(\mu_3\text{-O})(\text{H}_2\text{O})(\text{L-tartH})[\alpha\text{-P}_2\text{W}_{16}\text{O}_{59}]\cdot 18 \text{H}_2\text{O}$ : colorless needles, crystal size  $0.20 \times 0.04 \times 0.02 \text{ mm}^3$ ,  $\text{C}_{34}\text{H}_{161}\text{N}_{15}\text{O}_{141}\text{P}_4\text{W}_{31}\text{Zr}_3$ ,  $M_r = 9133.27$ , orthorhombic crystal system, space group  $P2_12_12_1$  (No. 19),  $a = 13.431(3)$ ,  $b = 33.897(7)$ ,  $c = 34.892(7)$  Å,  $V = 15885(6)$  Å<sup>3</sup>,  $Z = 4$ ;  $\rho_{\text{calcd}} = 3.674 \text{ g cm}^{-3}$ ;  $\mu(\text{MoK}\alpha) = 22.679 \text{ mm}^{-1}$ ;  $1.62 \leq \theta \leq 28.32^\circ$ . Data were collected with a Bruker SMART-APEX CCD sealed tube diffractometer with graphite monochromated  $\text{MoK}\alpha$  ( $\lambda = 0.71073$  Å) radiation. Data were measured using a series of combinations of  $\phi$  and  $\omega$  scans with 30 s frame exposures and  $0.3^\circ$  frames widths. The structure was solved by direct methods and refined by full-matrix least-squares against  $F^2$  of all data using SHELXTL software. Hydrogen atoms, except for the water hydrogen atoms, were included in calculated positions and assigned isotropic thermal parameters, riding on their parent carbon, oxygen or nitrogen atoms. The refinement converges with  $R_1 = 0.0941$  and  $wR_2 = 0.2247$  for 8472 reflections with  $I > 2\sigma(I)$ . The Flack parameter = 0.06(2) indicates the correct absolute configuration. Max/min residual electron density  $8.782/-3.863 \text{ e Å}^{-3}$ . The highest residual peaks are all associated with W atoms. CCDC 257975 (L-(–)-**1**) contains the supplementary crystallographic data for this paper. These data can be obtained free of charge from the Cambridge Crystallographic Data Centre via [www.ccdc.cam.ac.uk/data\\_request/cif](http://www.ccdc.cam.ac.uk/data_request/cif).

**1**:  $^{31}\text{P}$  NMR (162 MHz,  $\text{D}_2\text{O}$ ):  $\delta = -6.29, -6.62, -12.88, -13.83$  ppm; IR (KBr pellet, metal–oxygen stretching region):  $\tilde{\nu} = 1086$  (s), 1054 (sh), 1017 (m), 943 (s), 912 (s), 760 (s),  $697 \text{ cm}^{-1}$  (sh). The IR region for the tartrate ligand is not informative owing to its weak absorbance and overlap with that of the dimethyl ammonium counteranions. L-(–)-**1**:  $[\alpha]_{\text{D}}^{20} = -2.2$  ( $c = 1.0$  in  $\text{H}_2\text{O}$ );  $[M]_{\text{D}} = -200.9$ ; UV/Vis ( $\text{H}_2\text{O}$ ,  $2.2 \times 10^{-6} \text{ M}$ ):  $\lambda_{\text{max}} (\epsilon_{\text{max}}) = 196 (3.8 \times 10^5)$ , 280 nm ( $7.2 \times 10^4$ , sh); CD ( $\text{H}_2\text{O}$ ,  $c = 2.2 \times 10^{-4} \text{ M}$ , 0.1 cm cell): 241 ( $\theta = 25.1$ ,  $\Delta\epsilon = 35.3$ ), 270 ( $\theta = -4.8$ ,  $\Delta\epsilon = -6.7$ ), 285 ( $\theta = 4.9$ ,  $\Delta\epsilon = 6.9$ ), 309 nm ( $\theta = -8.6$ ,  $\Delta\epsilon = -12.0$ ). D-(+)-**1**:  $[\alpha]_{\text{D}}^{20} = 2.0$  ( $c = 1.0$  in  $\text{H}_2\text{O}$ );  $[M]_{\text{D}} = 183.9$ ; UV/Vis ( $\text{H}_2\text{O}$ ,  $2.2 \times 10^{-6} \text{ M}$ ):  $\lambda_{\text{max}} (\epsilon_{\text{max}}) = 196 (4.1 \times 10^5)$ , 280 nm ( $7.8 \times 10^4$ , sh); CD ( $\text{H}_2\text{O}$ ,  $c = 2.3 \times 10^{-4} \text{ M}$ , 0.1 cm cell): 239 ( $\theta = -27.0$ ,  $\Delta\epsilon = -36.0$ ), 268 ( $\theta = 5.9$ ,  $\Delta\epsilon = 7.9$ ), 285 ( $\theta = -4.2$ ,  $\Delta\epsilon = -5.7$ ), 312 nm ( $\theta = 9.2$ ,  $\Delta\epsilon = 12.1$ ).

Circular dichroism spectra were measured using a JASCO J-715 spectropolarimeter with 1 mm path-length cells. Spectra were collected between 190 and 600 nm, with a step size of 0.5 nm and at a speed of  $50 \text{ nm min}^{-1}$ . Three spectra were recorded and averaged automatically by the instrument. Optical rotations were measured on a Perkin Elmer 341 digital polarimeter with a 10 cm path-length cell.

Received: February 3, 2005

**Keywords:** chirality · circular dichroism · polyoxometalate · tartaric acid · zirconium

- [1] a) Topical issue on polyoxometalates (Guest Ed.: C. L. Hill), *Chem. Rev.* **1998**, 98, 1; b) *Polyoxometalate Chemistry: From Topology via Self-Assembly to Applications* (Eds.: M. T. Pope, A. Müller), Kluwer, Dordrecht, **2001**; c) *Polyoxometalate Chemistry for Nano-Composite Design* (Eds.: T. Yamase, M. T. Pope), Kluwer, Dordrecht, **2002**; d) “Polyoxo Anions: Synthesis and Structure”: M. T. Pope in *Comprehensive Coordination Chemistry II: Transition Metal Groups 3–6, Vol. 4* (Ed.: A. G. Wedd), Elsevier Science, New York, **2004**, chap. 4.10, pp. 635–678; e) “Polyoxometalates: Reactivity”: C. L. Hill in *Comprehensive Coordination Chemistry II: Transition Metal Groups 3–6, Vol. 4* (Ed.: A. G. Wedd), Elsevier Science, New York, **2004**, chap. 4.10, pp. 679–759.



- [2] a) R. Strandberg, *Acta Chem. Scand.* **1973**, 27, 1004; b) M. T. Pope, *Inorg. Chem.* **1976**, 15, 2008; c) A. Tézé, G. Hervé, *J. Inorg. Nucl. Chem.* **1977**, 39, 999; d) R. Contant, J. P. Ciabrini, *J. Chem. Res. Miniprint* **1977**, 2601; e) R. Acerete, J. Server-Carrió, A. Vegas, M. Martínez-Ripoll, *J. Am. Chem. Soc.* **1990**, 112, 9386; f) C. M. Tourné, G. F. Tourné, F. Zonnevillje, *J. Chem. Soc. Dalton Trans.* **1991**, 143; g) F. Xin, M. T. Pope, *J. Am. Chem. Soc.* **1996**, 118, 7731.
- [3] The Pfeiffer effect refers to the observation of induced circular dichroism (CD) signals for a configurationally labile chirality when the equilibrium between the enantiomers is shifted in presence of a chiral ligand. See: P. Pfeiffer, K. Quehl, *Ber. Dtsch. Chem. Ges. A* **1931**, 64, 2667; Pfeiffer effects in polyanion systems: a) J. F. Garvey, M. T. Pope, *Inorg. Chem.* **1978**, 17, 1115; b) K. Nomiya, R. Kobayashi, M. Miwa, *Bull. Chem. Soc. Jpn.* **1983**, 56, 3505. Since a Pfeiffer effect necessarily involves optical enrichment of polyanions under equilibrium conditions, this effect, alone, can not lead to isolation of bulk enantiomerically pure complexes, one goal and achievement of the present work.
- [4] Optical resolution of one enantiomer of a chiral polyanion: T. Ama, J. Hidaka, Y. Shimura, *Bull. Chem. Soc. Jpn.* **1970**, 43, 2654.
- [5] a) V. Soghomonian, Q. Chen, R. C. Haushalter, J. Zubieta, C. J. O'Connor, *Science* **1993**, 259, 1596; b) R. Knip, H. G. Will, I. Boy, C. Röhr, *Angew. Chem.* **1997**, 109, 1052; *Angew. Chem. Int. Ed. Engl.* **1997**, 36, 1013; c) T. E. Gier, X. Bu, P. Feng, G. D. Stucky, *Nature* **1998**, 395, 154; d) S. Neeraj, S. Natarajan, C. N. R. Rao, *Chem. Commun.* **1999**, 165; e) A. Yilmaz, X. Bu, M. Kizilyalli, G. D. Stucky, *Chem. Mater.* **2000**, 12, 3243; f) J. Liang, Y. Wang, J. Yu, Y. Li, R. Xu, *Chem. Commun.* **2003**, 882; g) Y. Wang, J. Yu, M. Guo, R. Xu, *Angew. Chem.* **2003**, 115, 4223; *Angew. Chem. Int. Ed.* **2003**, 42, 4089.
- [6] a) M. Inoue, T. Yamase, *Bull. Chem. Soc. Jpn.* **1995**, 68, 3055; b) U. Kortz, M. G. Savelieff, F. Y. A. Ghali, L. M. Khalil, S. A. Maalouf, D. I. Sinno, *Angew. Chem.* **2002**, 114, 4246; *Angew. Chem. Int. Ed.* **2002**, 41, 4070.
- [7] a) W. H. Knoth, R. L. Harlow, *J. Am. Chem. Soc.* **1981**, 103, 1865; b) M. J. Manos, H. N. Miras, V. Tangoulis, J. D. Woollins, A. M. Z. Slawin, T. A. Kabanos, *Angew. Chem.* **2003**, 115, 441; *Angew. Chem. Int. Ed.* **2003**, 42, 425; c) L. S. Felices, P. Vitoria, J. M. Gutiérrez-Zorrilla, S. Reinoso, J. Etxebarria, L. Lezama, *Chem. Eur. J.* **2004**, 10, 5138.
- [8] Kortz and Matta have demonstrated interpolyanion chirality in the trimeric complex,  $[(\beta_2\text{-SiW}_{11}\text{MnO}_{38}\text{OH})_3]^{15-}$ , which is present in an enantiomerically enriched (3:2) crystal. See U. Kortz, S. Matta, *Inorg. Chem.* **2001**, 40, 815.
- [9] POMs have a range of intriguing biological properties including potent antiviral activity: a) N. Fukuda, T. Yamase, *Biol. Pharm. Bull.* **1997**, 20, 927; b) J. T. Rhule, C. L. Hill, D. A. Judd, R. F. Schinazi, *Chem. Rev.* **1998**, 98, 327; c) J. T. Rhule, C. L. Hill, Z. Zheng, R. F. Schinazi, *Top. Biol. Inorg. Chem.* **1999**, 2, 117; d) D. A. Judd, J. H. Nettles, N. Nevins, J. P. Snyder, D. C. Liotta, J. Tang, J. Ermolieff, R. F. Schinazi, C. L. Hill, *J. Am. Chem. Soc.* **2001**, 123, 886; e) S. Shigeta, S. Mori, E. Kodama, J. Kodama, K. Takahashi, T. Yamase, *Antiviral Res.* **2003**, 58, 265.
- [10] ICD is realized when an achiral molecule(s) displays CD signals within their absorbing regions on association with a chiral inducer. For representative examples, see the recent review: S. Allenmark, *Chirality* **2003**, 15, 409.
- [11] A solid with one-dimensional helical strands constituted by L or D-tartrate,  $\text{Mo}_2\text{O}_4$ , and Gd has been reported. See a) C. Wu, C. Lu, X. Lin, D. Wu, S. Lu, H. Zhuang, J. Huang, *Chem. Commun.* **2003**, 1284; b) C. Wu, C. Lu, S. Lu, H. Zhuang, J. Huang, *Dalton Trans.* **2003**, 3192.
- [12] D. T. Richens, *The Chemistry of Aqua Ions*, Wiley, Chichester, **1997**.
- [13] Zirconium-containing polyanions are known: a) R. G. Finke, B. Rapko, T. J. R. Weakley, *Inorg. Chem.* **1989**, 28, 1573; b) L. Meng, J. F. Liu, *Transition Met. Chem.* **1995**, 20, 188; c) A. J. Gaunt, I. May, D. Collison, K. T. Holman, M. T. Pope, *J. Mol. Struct.* **2003**, 656, 101.
- [14] a) J. Gawroński, K. Gawrońska, *Tartaric and Malic Acids in Synthesis: A Source Book of Building Blocks, Ligands, Auxiliaries, and Resolving Agents*, Wiley-Interscience, New York, **1999**; b) S. F. Pedersen, J. C. Dewan, R. R. Eckman, B. K. Sharpless, *J. Am. Chem. Soc.* **1987**, 109, 1279.
- [15] The UV spectra of the plenary  $[\alpha\text{-P}_2\text{W}_{18}\text{O}_{62}]^{6-}$  and lacunary  $[\alpha_2\text{-P}_2\text{W}_{17}\text{O}_{61}]^{10-}$ ,  $[\alpha\text{-P}_2\text{W}_{15}\text{O}_{56}]^{12-}$  (freshly prepared) Wells–Dawson POMs have similar absorption bands up to approximately 330 nm, all displaying distinct maxima at around 195 nm and a broad shoulder of moderate intensity at about 280 nm.
- [16] J. Gawroński, J. Grajewski, *Org. Lett.* **2003**, 5, 3301.
- [17] The synthesis of  $\text{Na}_{12}[\alpha\text{-P}_2\text{W}_{15}\text{O}_{56}] \cdot 18\text{H}_2\text{O}$  was by the literature method: R. Contant, *Inorg. Synth.* **1990**, 27, 106.